

# Non-universal Efimov Atom-Dimer Resonances in a Three-Component Mixture of ${}^6\text{Li}$

Shuta Nakajima<sup>1\*</sup>, Munekazu Horikoshi<sup>2</sup>, Takashi Mukaiyama<sup>2,3</sup>, Pascal Naidon<sup>2</sup> and Masahito Ueda<sup>1,2\*</sup>

<sup>1</sup>*Department of Physics, University of Tokyo, 7-3-1, Hongo, Bunkyo-ku, Tokyo 113-0033, Japan*

<sup>2</sup>*ERATO Macroscopic Quantum Control Project, JST, 2-11-16 Yayoi, Bunkyo-ku, Tokyo 113-8656, Japan*

<sup>3</sup>*Center for Frontier Science and Engineering and Institute for Laser Science, University of Electro-Communications, 1-5-1 Chofugaoka, Chofu, Tokyo 182-8585, Japan.*

(Dated: September 26, 2018)

We observed an enhanced atom-dimer relaxation due to the existence of Efimov states in a three-component mixture of  ${}^6\text{Li}$  atoms. We measured the magnetic-field dependence of the atom-dimer loss coefficient in the mixture of atoms in state  $|1\rangle$  and dimers formed in states  $|2\rangle$  and  $|3\rangle$ , and found two peaks corresponding to the degeneracy points of the  $|23\rangle$  dimer energy level and energy levels of Efimov trimers. We found that the locations of these peaks disagree with universal theory predictions, in a way that cannot be explained by non-universal two-body properties. We constructed theoretical models that characterize the non-universal three-body physics of three-component  ${}^6\text{Li}$  atoms in the low energy domain.

Since the first experimental evidence of Efimov states [1] in an ultracold cesium atomic gas [2], few-body physics in ultracold atoms has attracted growing interest. The observation of three-body and atom-dimer loss peaks and dips confirmed very general properties of few-boson systems near unitarity such as the universal scaling laws associated with the existence of Efimov states [2–7]. Although these loss enhancements and recombination minima are qualitatively explained by the universal theory, their positions are shifted from universal predictions. While some efforts have been made to explain such resonance shifts by taking into account finite-range corrections [8–10], it is still an open question how accurately those corrections reproduce the observed Efimov spectra.

Recently, it has turned out that a three-component Fermi gas of  ${}^6\text{Li}$  offers another intriguing system to investigate universal few-body physics. Ottenstein *et al.* [11] and Huckans *et al.* [12] observed the enhancement of the three-body loss at 130 G and 500 G in the mixture of fermionic  ${}^6\text{Li}$  atoms in the three lowest-energy hyperfine states  $|F; m_F\rangle = |1/2; 1/2\rangle$ ,  $|1/2; -1/2\rangle$  and  $|3/2; -3/2\rangle$ , which we label as  $|1\rangle$ ,  $|2\rangle$  and  $|3\rangle$  respectively. Another resonance was later observed at 895 G [13]. It was argued that those three-body loss enhancements are due to the existence of Efimov states [14–18], as in the case of identical bosons. In such a system, however, because of their fermionic nature, only distinguishable particles can interact via s-wave scattering. Thus interactions for the respective combinations are described by three different two-body scattering lengths  $a_{12}$ ,  $a_{23}$  and  $a_{31}$ , which diverge at 834 G, 811 G, and 690 G respectively due to Feshbach resonances (see Fig. 1(a)). For each of these resonances there is a weakly bound dimer state which we designate as  $|12\rangle$ ,  $|23\rangle$  and  $|31\rangle$ , respectively (see Fig. 1(b)). Because these Feshbach resonance regimes overlap, the three scattering lengths can be varied simultaneously with a magnetic field, making it possible to realize a strongly-interacting multi-component system and access a whole new quantum phase of matter [19]. For this purpose, an accurate understanding

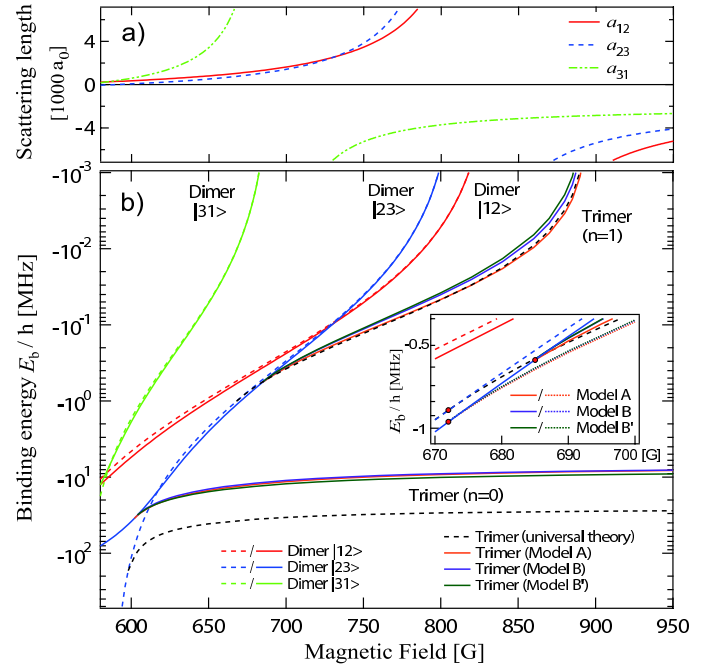


FIG. 1. (a) Two-body s-wave scattering lengths in  ${}^6\text{Li}$  for states  $|1\rangle$ ,  $|2\rangle$ , and  $|3\rangle$  [20]. (b) Binding energies  $E_b$  of the dimer and trimer states in three-component mixture of  ${}^6\text{Li}$ . Dashed curves represent the energies from universal theory. Solid curves for dimers are obtained from two-body coupled-channel calculations. Solid curves for trimers are obtained from our non-universal models adjusted to the experimental data. The inset shows the dimer-trimer crossing near 685 G. Dotted lines correspond to non-universal models without adjustment of the three-body parameter.

of the low-energy few-body physics is necessary. As in the case of identical bosons, this requires an accurate determination of the Efimov spectrum.

In this Letter, we report the observation of two resonantly enhanced atom-dimer loss peaks in an atom-dimer mixture of  ${}^6\text{Li}$  corresponding to the degeneracy points be-

tween the binding energy of  $|23\rangle$  dimers and the ground ( $n = 0$ ) and excited ( $n = 1$ ) Efimov trimer states (see Fig. 1(b)). These peaks have been predicted by Braaten *et al.* from theory based on universality [18]. We compare the observed peak positions with universal theory predictions, and find significant deviations which cannot be explained by two-body physics only. We then construct non-universal models to interpret them.

In our experiment we used an all-optical method to prepare a degenerate two-component Fermi gas of  ${}^6\text{Li}$  atoms in the two lowest hyperfine states of  $|1\rangle$  and  $|2\rangle$  as described in detail in [21]. To prepare a mixture of  $|1\rangle$  atoms and  $|23\rangle$  dimers in equal population, we started with an imbalanced mixture of atoms in state  $|1\rangle$  and  $|2\rangle$  whose population ratio is  $|1\rangle : |2\rangle = 2 : 1$ . Evaporative cooling was performed at the magnetic field of 300 G where the amplitude of the scattering length between  $|1\rangle$  and  $|2\rangle$  shows a local maximum. The total number of atoms before dimer creation was  $\sim 10^6$ . To achieve a very low collision energy, we adiabatically transferred this mixture into a larger volume hybrid magnetic/optical trap with smaller oscillation frequencies. The trap frequencies for atoms  $\omega^A$  were experimentally measured and approximately given by  $\omega_x^A = 2\pi \times \sqrt{110^2 - 0.73B}$  Hz,  $\omega_y^A = 2\pi \times \sqrt{50^2 - 0.31B}$  Hz and  $\omega_z^A = 2\pi \times \sqrt{7.2^2 + 0.45B}$  Hz in  $x, y$  and  $z$  directions respectively, where  $B$  is the strength of magnetic field in Gauss. Since the magnetic moments of  $|1\rangle$  atoms and  $|23\rangle$  dimers are different, the trap frequencies for dimers  $\omega^D$  are different from the ones for  $|1\rangle$  atoms, especially below 650 G. The trap frequencies for dimers were calculated using the magnetic moment of  $|23\rangle$  dimers. Deviation of  $\omega^D$  from the  $\omega^A$  for  $x, y$  and  $z$  directions at 580 G were about +6, +27, -26 % respectively.

To create the atom-dimer mixture, we used a multiple-stage adiabatic rapid passage (ARP) as shown in Fig. 2(a). By applying ARP at 563 G, we first transferred the atoms in state  $|2\rangle$  to state  $|3\rangle$ . Then we transferred the atoms in state  $|1\rangle$  to state  $|2\rangle$  by ARP. Thus we created an imbalanced mixture of  $|2\rangle$  and  $|3\rangle$  whose population ratio is  $|2\rangle : |3\rangle = 2 : 1$ . After the preparation of the imbalanced  $|2\rangle - |3\rangle$  mixture, we quickly ramped the magnetic field up to 811 G, and then swept down to the field of interest (580 G-760 G) in 300 ms to adiabatically create  $|23\rangle$  dimers. At this point, excess atoms in state  $|2\rangle$  were still left in the trap and the last stage of ARP was applied to transfer the atoms in state  $|2\rangle$  to state  $|1\rangle$  to obtain a  $|1\rangle$  atom -  $|23\rangle$  dimer mixture.

To study the decay of an atom-dimer mixture, we measured the remaining fraction of atoms in  $|1\rangle$  after a holding time of 1 ~ 1000 ms. The magnetic-field dependence of the atom-dimer loss rate was measured by repeating this sequence with various magnetic field values. Therefore the last stage of ARP was applied at a different magnetic field, and the condition for perfect ARP was checked at each magnetic field. When we take the absorption images, we

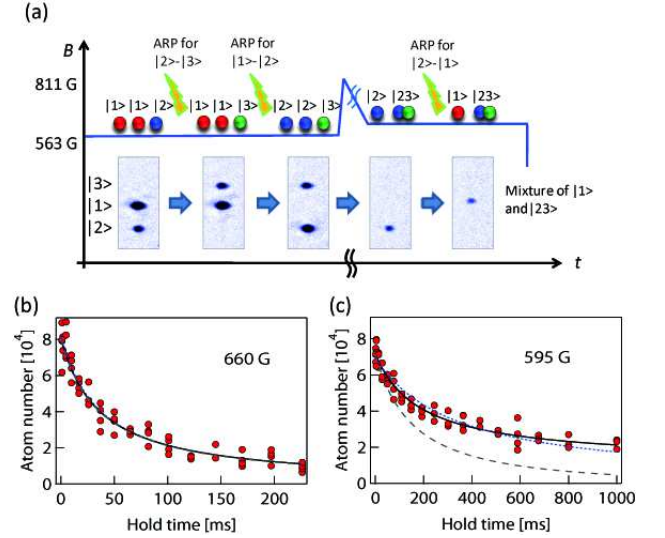


FIG. 2. (a) Experimental procedure to prepare atom-dimer mixtures by using a multiple-stage adiabatic rapid passage (see text). Because the dimers cannot be imaged by resonance light, we dissociate the dimers by applying a magnetic field pulse to check the population balance of the atoms and dimers. (b) and (c): Typical time evolution of the number of atoms in state  $|1\rangle$  at 660 G and 595 G. The blue dotted curve shows an analytic fitting function assuming the pure two-body loss and the black solid curve is obtained by a numerical fitting that includes the effect of dimer-dimer loss. Gray dashed curves show time evolution of the numbers of molecules calculated from the rate equations.

pulsed on the magnetic field gradient and spatially separated each spin component. This allowed us to check that there was no excess atoms in states  $|2\rangle$  and  $|3\rangle$  during the loss measurements. Although the temperature of the atom-dimer mixture is very low ( $\sim 100$  nK), it is close to the Fermi temperature due to the very low density. Therefore, we assume that the density distributions of atoms and dimers are Gaussian. Then, the number of atoms  $N_A(t)$  and that of dimers  $N_D(t)$  evolve in time according to the following coupled rate equations,

$$\dot{N}_A = -\Gamma N_A - C\beta \frac{N_D}{V_D} N_A, \quad (1)$$

$$\dot{N}_D = -\Gamma N_D - C\beta \frac{N_A}{V_A} N_D - \alpha \frac{N_D}{V_D} N_D, \quad (2)$$

where  $\beta$ ,  $\alpha$  and  $\Gamma^{-1} = 10$  s are the atom-dimer loss coefficient, the dimer-dimer loss coefficient and the one-body loss rate, respectively. Here,  $V_A = \sqrt{8\pi^{\frac{3}{2}} \sigma_x^A \sigma_y^A \sigma_z^A}$  and  $V_D = \sqrt{8\pi^{\frac{3}{2}} \sigma_x^D \sigma_y^D \sigma_z^D} = V_A (\bar{\omega}^A / \sqrt{2} \bar{\omega}^D)^3$  are the effective atomic and molecular volumes, where  $\sigma_{x,y,z}^A = \sqrt{k_B T / m (\omega_{x,y,z}^A)^2}$  and  $\sigma_{x,y,z}^D = \sqrt{k_B T / 2m (\omega_{x,y,z}^D)^2}$  are the atomic and dimer cloud widths. We denote the mass of  ${}^6\text{Li}$  by  $m$ , and  $\bar{\omega}^A$  and  $\bar{\omega}^D$  are the geometric means of the trap frequencies for atoms and dimers.  $C = \prod_i \sqrt{4 / (2 + (\omega_i^A / \omega_i^D)^2)} \simeq 8 / \sqrt{27}$  is a numerical con-

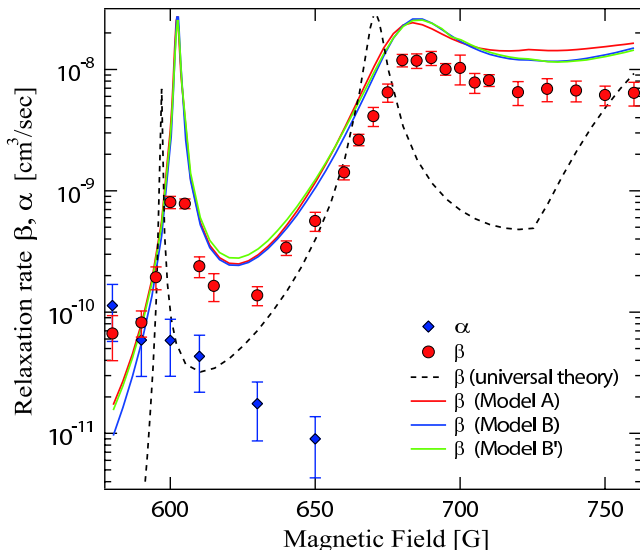


FIG. 3. Magnetic-field dependence of the atom-dimer loss coefficient  $\beta$  (red circles) and dimer-dimer loss coefficient  $\alpha$  (blue diamonds) in the mixture of atoms in state  $|1\rangle$  and dimers of  $|23\rangle$ . The black dashed curve is the calculated  $\beta$  from universal theory. Red, blue, and green solid curves show the  $\beta$  values calculated from our non-universal models A, B and B' respectively.

stant which results from the difference of the density distributions of the atoms and dimers due to unequal masses [6].

We determined the atom-dimer loss coefficient  $\beta$  by fitting our data with the solution of the rate equations using  $\Gamma$  and  $\alpha$  which were experimentally determined in advance. We checked that the cloud size remains approximately constant; therefore we assume the constant volume and ignore heating effect in our analysis. We found that the decay time scale of atom-dimer loss above 650 G is far shorter than the time scales of dimer-dimer and one-body loss and the decay curve can be described using two-body loss fitting. However, below 650 G, the dimer-dimer loss and one-body loss need to be taken into account (see Fig. 2(b) and (c)).

Figure 3 shows the measurement of the atom-dimer loss coefficient  $\beta$  (red circles) and the dimer-dimer loss coefficient  $\alpha$  (blue diamonds) for the  $|23\rangle$  dimers, as a function of magnetic field. The error bars for  $\alpha$  show the systematic error of our measurements arising from the uncertainty in the number of atoms and size measurements. The error bars for  $\beta$  arise from the statistical error of size measurements and error propagation of  $\alpha$ . The systematic error arising from the uncertainty in the number of atoms, which is estimated to be  $\pm 22\%$  and may shift the data linearly, is not included in these error bars. We observe two maxima of the atom-dimer loss coefficient near 602 G and 685 G.

The atom-dimer loss is expected to increase at the magnetic field where the energy level of an Efimov state intersects with the energy level of the  $|23\rangle$  dimer [18]. Since there is no other mechanism that causes an enhanced atom-

dimer loss, the two peaks observed in Fig. 3 should correspond to such Efimov resonances. Because the lower peak is expected to be associated with a “ground-state” Efimov trimer, our finding provides the first experimental evidence for this “ground-state” Efimov trimer in the three-component mixture of  $^6\text{Li}$ .

We now analyze the data. The usual universal theory [15, 16, 18] for this kind of three-body systems relies only on the 3 scattering lengths to describe the two-body interactions and a short-range three-body parameter  $\Lambda e^{i\eta}$ , where  $\Lambda$  fixes the phase of the three-body wave function at short distance and  $\eta > 0$  phenomenologically models losses occurring when 3 atoms come close. These free parameters were previously determined to be  $\Lambda = 0.885 a_0^{-1}$  and  $\eta = 0.016$  from the zero-energy resonance at 895 G lying right in the universal region of large scattering lengths. Figures. 1(b) and 3 show the universal predictions for the trimer energy and atom-dimer loss coefficient using these previously determined parameters. While they qualitatively explain the presence of the two resonances, there is significant disagreement. This is not surprising because the resonances investigated here are significantly away from the universal region. Near the resonance at 602 G, the scattering lengths are on the order of the range of the interactions (the van der Waals length  $\ell_{vdW} \sim 60 a_0$ ) and the binding energy of  $|23\rangle$  dimers differs by 57 % from the universal form  $-\hbar^2/ma_{23}^2$ . Near the resonance at 685 G, the scattering lengths are much larger, yet the binding energy still differs from the universal form by 8 %. If we follow the predicted universal trimer energy, this deviation suggests that the resonance point should be shifted to 685 G, which is interestingly very close to the observed peak location.

To check this point and make a consistent analysis of our data, the minimal requirement is to design a theory which accurately describes the non-universal two-body physics, in particular the dimer energies. The most straightforward way to achieve this is to solve the three-body problem with zero-range interactions parametrized by energy-dependent scattering lengths. This can be easily implemented using the Skorniakov - Ter-Martirosian coupled integral equations [18, 23, 24]. The scattering length  $a(k)$  should accurately reproduce the asymptotic two-body physics at positive and negative energies  $E = \frac{\hbar^2 k^2}{m}$ . In particular, the dimer binding energy  $E_b = -\frac{\hbar^2 \kappa^2}{m}$  is given by  $1/a(i\kappa) = \kappa$ . The universal limit is retrieved for an energy-independent scattering length  $1/a(k) = 1/a$ . A realistic analytical expression near a Feshbach resonance can be derived from a two-channel model, for instance with separable Gaussian interactions [10]. It leads to

$$\frac{1}{a(ik)} = e^{-(bk)^2} \frac{1}{a_{bg}} \left( 1 - \frac{1}{(k\sigma(B))^2 + \frac{B-B_0}{\Delta(B)}} \right)^{-1} + f(k)$$

where the first term contains the resonance parameters  $a_{bg}$ ,  $B_0$ ,  $\Delta(B)$ , and  $\sigma(B)$  which are fitted to reproduce accu-

rately the zero-energy scattering length, the effective range, and the last dimer binding energy - all obtained from a two-body coupled-channel calculation for each hyperfine configuration. The high-energy term  $f(k)$  is found to be  $f_A(k) = k\text{Erf}(kb)$  which behaves as  $k$  at large  $k$ . While the high-energy (short-distance) behaviour is irrelevant for the low-energy two-body physics, it does change the three-body phase at short distance. It is known however that two-body physics only cannot determine that phase in general [22]. Although we could adjust the high-energy two-body form to effectively set the 3-body phase [10], we rely for that purpose on the three-body parameter  $\Lambda e^{i\eta}$ , which appears as an upper bound of the integral in the STM equations. To check that our theory does not depend on the two-body high-energy form, we consider an alternative form  $f_B(k) = \frac{bk^2}{1+(bk)^2}$  which tends to a constant  $\frac{1}{b}$  at large  $k$ . In all cases, we choose a form which is independent of the low-energy parameters, and is therefore magnetic-field independent.

Using these two models, which we refer to A and B, we first adjust the three-body parameters  $\Lambda$  and  $\eta$  to fit the previously measured loss coefficient near the zero-energy resonance at 895 G. As in the usual Efimov theory, the choice of  $\Lambda$  is not unique and for completeness we consider two values for model B, which we refer to B and B'. We found that all models yield exactly the same universal resonant loss profile near 895 G. Using those parameters, we then investigate the atom-dimer properties. All models give essentially the same prediction for the second resonance near at 685 G, but different ones for the first resonance at 602 G, probably reflecting its strongly non-universal character. The predicted location of the second resonance is around 672 G (see inset of Fig. 1), which is not shifted from the universal prediction as we naively expected - we also checked that the same result is obtained with a simple effective range model. We conclude that our experimental data show that the short-range physics parametrization cannot be constant altogether. Therefore, if we keep our two-body parametrization, the three-body parameter  $\Lambda$  must depend on energy, and possibly magnetic field. This seems reasonable, since the two-body parameters  $a(k)$  are already required to be energy-dependent in order to describe the non-universal two-body physics.

We proceed to map out this energy dependence by fitting each resonance with our models - see Table I. The variation of  $\Lambda$  with magnetic field is smooth and almost linear, but it corresponds to a non linear dependence on energy. The variation of  $\eta$  is not monotonic and varies over one order of magnitude. This is not totally unexpected since it describes underlying loss processes which are at present unknown. We then perform a quadratic fit for both  $\Lambda$  and  $\ln \eta$  to estimate those parameters at any magnetic field, and plot the corresponding atom-dimer loss coefficients for each model, as well as the Efimov trimer energies - see Figs. 1(b) and 3. The results are essentially the same, indicating that our

TABLE I. Fitted three-body parameters  $\Lambda$  and  $\eta$  for different magnetic fields (energies) corresponding to different resonant points. These values are obtained for  $b = 38.85 a_0$  in Model A, and  $b = 43.93 a_0$  in Model B and B', which best reproduce the effective ranges of the interactions. We assume that the values for  $\Lambda$  are the same at zero energy.

Model	602 G	685 G	810 G ( $E = 0$ )	895 G ( $E = 0$ )
A	$\Lambda=0.0405$	$\Lambda=0.0460$	$\Lambda=0.0484$	$\Lambda=0.0484$
B	$\Lambda=0.0111$	$\Lambda=0.0152$	$\Lambda=0.0186$	$\Lambda=0.0186$
B'	$\Lambda=0.141$	$\Lambda=0.185$	$\Lambda=0.244$	$\Lambda=0.244$
A	$\eta=0.008$	$\eta=0.08$	-	$\eta=0.033$
B	$\eta=0.020$	$\eta=0.20$	-	$\eta=0.011$
B'	$\eta=0.035$	$\eta=0.30$	-	$\eta=0.016$

analysis is model-independent. It reproduces the experimental data for  $B > 610$  G up to a factor of 2. The first resonance cannot be very well reproduced, most probably because it is located at an energy which lies at the margin of validity of our zero-range calculation.

In summary, we have measured the atom-dimer loss coefficient  $\beta$  in a mixture of  $^6\text{Li}$  hyperfine state  $|1\rangle$  and  $^6\text{Li}$  dimers in state  $|23\rangle$ , and found two loss maxima near 602 G and 685 G. We attributed these peaks to the crossings between the atom-dimer threshold and two (ground and excited) Efimov states. We found significant deviations from the universal predictions, and showed that they cannot be explained simply by taking into account the non-universal two-body physics. Our work therefore provides evidence for the non-universal character of short-range three-body behaviour, which we quantified by variations of the three-body short-range parameters. Although these parameters are different for different two-body models, they lead to a model-independent interpretation of our data, which predicts the non-universal properties of the two Efimov trimers in three-component  $^6\text{Li}$ . Understanding these three-body short-range variations will be a challenging task in the future.

During the preparation of this paper, we became aware of similar results reported by T. Lompe et al. [25].

We thank Y. Castin and L. Pricoupenko for useful discussions, and P. S. Julienne and E. Tiesinga for providing accurate lithium interaction potentials. S.N. acknowledges support from the Japan Society for the Promotion of Science.

---

\* shuta@cat.phys.s.u-tokyo.ac.jp

- [1] V. Efimov, Sov. J. Nucl. Phys. **12**, 589 (1971) ; V. Efimov, Nucl. Phys. A, **210**, 157 (1973).
- [2] T. Kraemer *et al.*, Nature (London) **440**, 315 (2006).
- [3] M. Zaccanti *et al.*, Nature Physics **5**, 586 (2009).
- [4] N. Gross, Z. Shotan, S. Kokkelmans, and L. Khaykovich, Phys. Rev. Lett. **103**, 163202 (2009).
- [5] S. E. Pollack, D. Dries, and R. G. Hulet, Science **326**, 1683

- (2009).
- [6] S. Knoop *et al.*, Nature Physics **5**, 227 (2009).
  - [7] G. Barontini *et al.*, Phys. Rev. Lett.**103**, 043201 (2009).
  - [8] H.-W. Hammer, T. A. Lähde, and L. Platter, Phys. Rev. A **75**, 032715 (2007).
  - [9] M. Thøgersen, D. V. Fedorov, and A. S. Jensen, Phys. Rev. A **78**, 020501(R) (2008).
  - [10] M. Jona-Lasinio and L. Pricoupenko, Phys. Rev. Lett.**104**, 023201 (2010).
  - [11] T. B. Ottenstein, T. Lompe, M. Kohnen, A. N. Wenz and S. Jochim, Phys. Rev. Lett.**101**, 203202 (2008).
  - [12] J. H. Huckans, J. R. Williams, E. L. Hazlett, R. W. Stites and K. M. OHara, Phys. Rev. Lett.**102**, 165302 (2009).
  - [13] J. R. Williams *et al.*, Phys. Rev. Lett.**103**, 130404 (2009).
  - [14] S. Floerchinger, R. Schmidt, and C. Wetterich, Phys. Rev. A **79**, 053633 (2009).
  - [15] E. Braaten, H.-W. Hammer, D. Kang and L. Platter, Phys. Rev. Lett.**103**, 073202 (2009).
  - [16] P. Naidon and M. Ueda, Phys. Rev. Lett.**103**, 073203 (2009).
  - [17] A. N. Wenz *et al.*, Phys. Rev. A **80**, 040702(R) (2009).
  - [18] E. Braaten, H.-W. Hammer, D. Kang and L. Platter, Phys. Rev. A. **81**, 013605 (2010).
  - [19] P. F. Bedaque and J. P. D’Incao, Ann. of Phys. **324**, 1763 (2009).
  - [20] M. Bartenstein *et al.*, Phys. Rev. Lett.**94**, 103201 (2005).
  - [21] Y. Inada *et al.*, Phys. Rev. Lett.**101**, 180406 (2008).
  - [22] J. P. D’Incao, C. H. Greene, and B. D. Esry, J. Phys. B **42**, 044016 (2009).
  - [23] G. V. Skorniakov and K. A. Ter-Martirosian, Sov. Phys. JETP **4**, 648 (1957).
  - [24] V. Efimov, Phys. Rev. C, **44**, 2303 (1991)
  - [25] T. Lampe *et al.*, arXiv:1003.0600 (2010).